PROCEEDINGS OF SCIENCE

Production of (anti)(hyper)nuclei at the LHC with ALICE

Luca Barioglio* on behalf of the ALICE Collaboration

Technische Universität München,
Physik Department, James-Franck-Straße 1, 85748 Garching bei München, Germany

E-mail: luca.barioglio@cern.ch

The production mechanism of light (anti)nuclei and (anti)hypernuclei in hadron collisions is still under debate in high-energy physics. Two different classes of phenomenological models are used to describe the (hyper)nuclear production: the statistical hadronisation model and the coalescence model. Thanks to its excellent particle-identification capabilities, ALICE is the best experiment at the LHC for the measurement of (hyper)nuclei. During the LHC Run 1 and Run 2, ALICE has measured the production of (anti)(hyper)nuclei in pp, p–Pb and Pb–Pb collisions at different energies. For the first time it has been possible to measure hypertriton production in pp and p–Pb collisions. In the following, the latest results on the measured production of (anti)(hyper)nuclei is compared with the predictions of the coalescence model and of the statistical hadronisation model, in order to understand which of the two provides the best description.

The Ninth Annual Conference on Large Hadron Collider Physics - LHCP2021
7-12 June 2021
Online

PoS(LHCP2021)056

1. Nuclear matter production

The study of the production of light (anti)(hyper)nuclei is an extremely interesting and important topic in high-energy physics. Although light (anti)(hyper)nuclei are abundantly produced in hadron collisions at the LHC, their production mechanism is still debated. Two classes of phenomenological models are available, namely the statistical hadronisation model (SHM) [1] and the coalescence model [2].

On the one hand, in the frame of the SHM (anti)nuclei and (anti)hypernuclei are produced at the chemical freeze-out in statistical equilibrium, along with all the other hadrons. Using only three parameters (temperature T, volume V and baryon chemical potential μ_B), the SHM can describe the production yields ($\mathrm{d}N/\mathrm{d}y$) of hadrons and nuclei in central Pb–Pb collisions over nine orders of magnitude [3]. Large colliding systems as Pb–Pb are described within the grand canonical (GC) ensemble and this assumption is valid because the volume of the fireball is large enough to fulfil the condition $VT^3 > 1$, where V and T are the system volume and temperature, respectively. On the contrary, pp and p–Pb collisions are characterised by a smaller volume and a canonical description if the system is necessary. The predictions obtained with the canonical statistical model (CSM) tend to those obtained with the grand canonical one as the system size increases from pp to Pb–Pb collisions. The CSM predictions here presented are obtained from the THERMAL-FIST package [4], in which baryon number, strangeness content and electric charge are exactly conserved.

In the coalescence picture, nucleons that are close to each other in phase space can form a nucleus via coalescence [2]. The key concept is the overlap between the nuclear wave function and the phase space of the constituent nucleons. The main observable of the model is the coalescence parameter, defined as:

$$B_A\left(p_{\mathrm{T}}^{\mathrm{p}}\right) = \frac{1}{2\pi p_{\mathrm{T}}^{\mathrm{A}}}\frac{\mathrm{d}^2 N_{\mathrm{A}}}{\mathrm{d}y\mathrm{d}p_{\mathrm{T}}^{\mathrm{A}}} \Bigg/ \left(\frac{1}{2\pi p_{\mathrm{T}}^{\mathrm{p}}}\frac{\mathrm{d}^2 N_{\mathrm{p}}}{\mathrm{d}y\mathrm{d}p_{\mathrm{T}}^{\mathrm{p}}}\right)^A \tag{1}$$

where the invariant spectra $\frac{1}{2\pi p_{\mathrm{T}}}\frac{\mathrm{d}^2 N}{\mathrm{d}y\mathrm{d}p_{\mathrm{T}}}$ of the (anti)protons are evaluated at the transverse momentum p_{T} of the nucleus divided by its mass number A, so that $p_{\mathrm{T}}^{\mathrm{p}} = p_{\mathrm{T}}^{\mathrm{A}}/A$. The coalescence parameter is related to the probability of forming a nucleus via coalescence [2].

In order to study the dependence of the production mechanisms on the system size, the measurements are carried out as a function of the averaged charged-particle multiplicity rapidity density (hereinafter just called multiplicity) measured at midrapidity $\langle \mathrm{d}N_{\mathrm{ch}}/\mathrm{d}\eta \rangle$. By considering the measurement of the source radius obtained through femtoscopy measurements in different collision systems and for different multiplicity classes, it is possible to correlate the system size to $\langle \mathrm{d}N_{\mathrm{ch}}/\mathrm{d}\eta \rangle$ [5].

2. Results

The evolution of B_A as a function of multiplicity is shown in Fig. 1, for (anti)deuterons (left) and for (anti)helion (right), respectively. B_2 is evaluated at $p_{\mathrm{T}}/\mathrm{A}$ = 0.75 GeV/c, while B_3 at $p_{\mathrm{T}}/\mathrm{A}$ = 0.90 GeV/c. A similar trend is obtained for other values of $p_{\mathrm{T}}/\mathrm{A}$. Data are compared with the theoretical predictions for the coalescence model [5], using two different parameterisations of

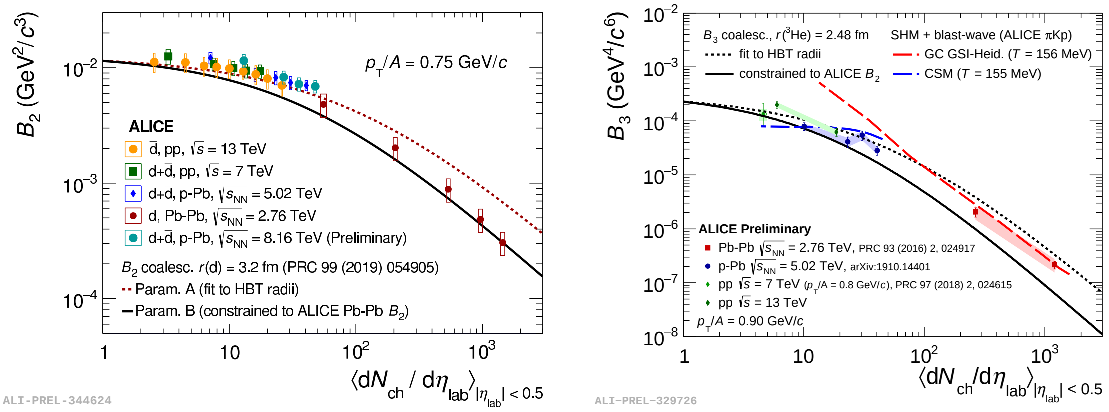

Figure 1: B_2 (left) and B_3 (right) as a function of charged-particle multiplicity $\langle dN_{ch}/d\eta \rangle$ at p_T/A = 0.75 GeV/c and p_T/A = 0.90 GeV/c, respectively. Data are compared with the predictions of the coalescence model [5]. The dashed line (red for B_2 and black for B_3) and the black continuous one correspond to different parameterisations of $\langle dN_{ch}/d\eta \rangle$ with respect to the HBT radius. B_3 is also compared with the predictions of thermal model (coloured dashed lines) [1].

the system radius as a function of multiplicity. The data show a smooth evolution as a function of multiplicity, suggesting a common production mechanism that depends only on the system size. The observed trend is an effect of the interplay between the size of the nucleus and the one of the colliding system. For pp and p–Pb collisions the system size is smaller than the nuclear size and B_A slightly decreases with multiplicity. On the contrary, for Pb–Pb collision the system size is sensibly larger than the nucleus size and therefore the decrease of B_A with multiplicity is more important. As it can be observed in the figure, the general trend is reproduced by the coalescence model. Moreover, B_3 is also compared with the predictions of SHM: for Pb–Pb collisions, the trend is qualitatively described by a GC SHM, but the CSM fails in reproducing the B_3 in small systems.

Fig. 2 shows the ratio between the p_T-integrated yields of nuclei and protons for deuterons (d/p), ^{3}He (^{3}He/p) and ^{3}H (H/p). Data are compared with the CSM predictions and with coalescence calculations [6]. For ^{3}He, results from both the two-body and the three-body coalescence are reported. Predictions for ^{3}H are not shown, because they are very similar to those for ^{3}He [7]. As already observed for B_A, the smooth evolution of the data with multiplicity suggests a common mechanism that depends only on the system size. Within the frame of the CSM, the rise at low multiplicity, i.e. for a small system radius, is an effect of the local conservation of quantum numbers (canonical suppression). With the increase of the system size, the canonical suppression gets released. Both the CSM and coalescence model describe the observed trend with multiplicity, even though for ^{3}He /p tensions between data and models are present.

Finally, the measurement of hypertriton in small systems provides a more decisive test for the production models. The reason is that the hypertriton radius ($r(^3_\Lambda\mathrm{H})$ = 10.79 fm [8]) is sensibly larger than the deuteron one ($r(\mathrm{d})$ = 3.2 fm [8]), leading to marked differences between the CSM and the coalescence model predictions at low multiplicity. Fig. 3 shows the measurement of the ratio between the p_T-integrated yields of hypetritons and Λ hyperons and of $S_3 = \left(^3_\Lambda\mathrm{H}/^3\mathrm{He}\right)/(\Lambda/\mathrm{p})$. Both the observables are compared with the predictions of the CSM and of the coalescence model.

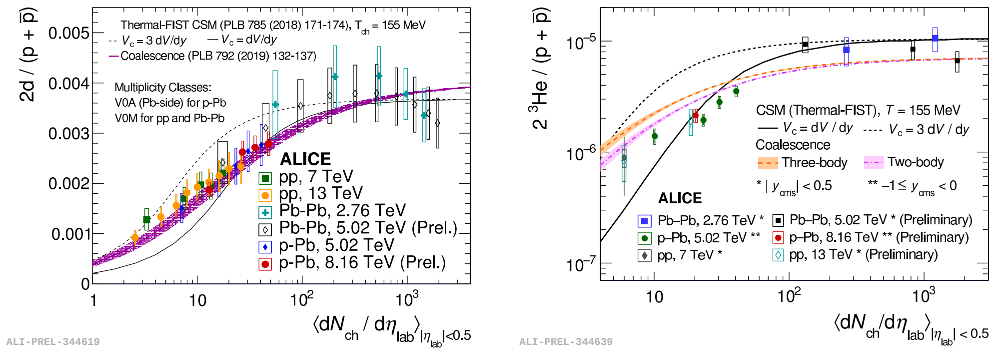

Figure 2: Ratio between the p_{T}-integrated yields of nuclei and protons for deuterons (d/p) (left), ^{3}He (^{3}He /p) and ^{3}H (^{3}H/p) (right). Data are compared with the predictions of the THERMAL-FIST CSM [4] and the coalescence model [6].

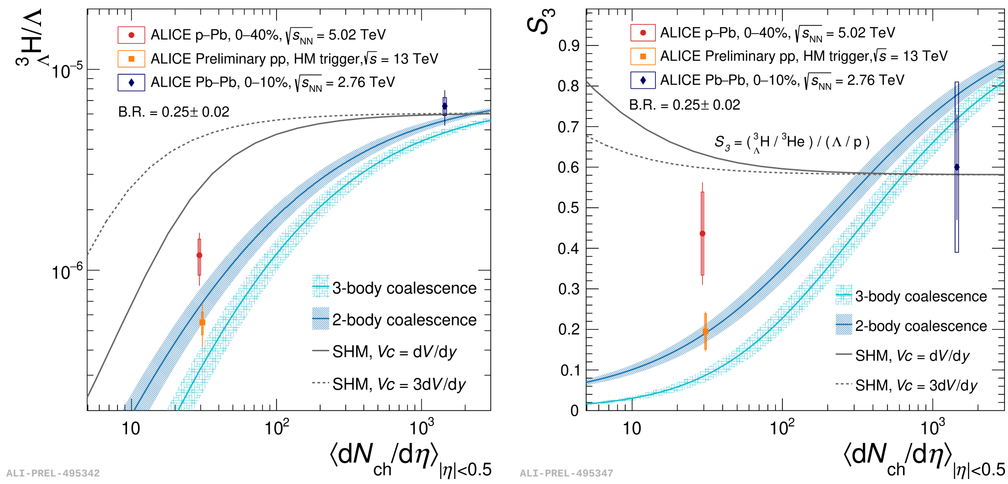

Figure 3: Ratio between the p_{T}-integrated yields of hypetritons and lambdas (left) and S_3 (right). Data are compared with the predictions of the CSM [4] and the coalescence model [6].

The measurements in pp and p–Pb collisions favour production via two-body coalescence.

3. Conclusions

The measurements of the coalescence parameter B_{A} and of the ratios between the p_{T}-integrated yields of light nuclei and protons show the presence of a common production mechanism that depends on the system size. Both the CSM and the coalescence model can describe the observed trend as a function of multiplicity, even though there are more tensions between data and models for helions than for deuterons. By considering the hypertriton production, it is possible to discern between the two mechanisms, due to the dependence of the coalescence model on the radius of the (hyper)nuclear cluster. Ratios of yields and S_3 at low multiplicity favour a production via two-body coalescence. With the LHC Run 3, thanks to the improved tracking precision and to the increased integrated luminosity, it will be possible to obtain more precise measurements and to further constrain the mechanism of (hyper)nuclear production.

References

[1] A. Andronic, P. Braun-Munzinger, J. Stachel and H. Stocker, *Production of light nuclei, hypernuclei and their antiparticles in relativistic nuclear collisions*, Phys. Lett. B **697** (2011) 203 [1010.2995].

[2] J.I. Kapusta, *Mechanisms for deuteron production in relativistic nuclear collisions*, Phys. Rev. C **21** (1980) 1301.

[3] ALICE collaboration, *Production of ^{4}He and $^{4}\overline{\text{He}}$ in Pb-Pb collisions at $\sqrt{s_{\rm NN}}$ = 2.76 TeV at the LHC*, Nucl. Phys. A **971** (2018) 1 [1710.07531].

[4] V. Vovchenko, B. Dönigus and H. Stoecker, *Multiplicity dependence of light nuclei production at LHC energies in the canonical statistical model*, Phys. Lett. **B785** (2018) 171 [1808.05245].

[5] F. Bellini and A.P. Kalweit, *Testing production scenarios for (anti-)(hyper-)nuclei and exotica at energies available at the cern large hadron collider*, Phys. Rev. C **99** (2019) 054905.

[6] K.-J. Sun, C.M. Ko and B. Dönigus, *Suppression of light nuclei production in collisions of small systems at the Large Hadron Collider*, Phys. Lett. B **792** (2019) 132 [1812.05175].

[7] ALICE collaboration, *Production of (anti-)^{3}He and (anti-)^{3}H in p-Pb collisions at $\sqrt{s_{\rm NN}}$ = 5.02 TeV*, Phys. Rev. C **101** (2020) 044906 [1910.14401].

[8] F. Hildenbrand and H.W. Hammer, *Three-Body Hypernuclei in Pionless Effective Field Theory*, Phys. Rev. C **100** (2019) 034002 [1904.05818].